Chapter 4

Zinc oxide coated Metal-Semiconductor-Metal based Biosensing Device

Chapter 4

Zinc oxide coated Metal-Semiconductor-Metal based Biosensing Device

4.1 Outline

The unique physicochemical and topological properties of n-type semiconducting zinc oxide (ZnO) thin film have been extensively explored in the field of optoelectronics, energy storage applications, and also for various biomedical applications such as biomaterials, biosensor, drug delivery system etc [212], [213]. When the surface of ZnO is exposed to any particular external environment, the variation in electron charge-transfer is detected either in the form of change in resistance, capacitance or impedance due to change in their dielectric properties, bulk electron mobility, grain boundaries, bulk oxide material, etc [148]. ZnO has a wide direct band gap of ~3.3 eV at a room temperature and also has a large exciton binding energy of ~60 meV. In addition, ZnO has high electron concentration, resulting to large conductivity, high redox potential, high transparency in optical region, and high resistance to radiation at a room temperature. Further, ZnO have shown to have high chemical and thermal stability with biocompatible nature [141], [149], [213], [214].

In this study, we have fabricated metal-semiconductor-metal (MSM) structured biosensor for the first time to monitor the dynamic behaviour of adherent mammalian cells. The n-type ZnO was synthesized *via* sol-gel technique and ZnO thin film was formed using the low-cost spin coating technique. ZnO thin films were functionalized with gelatin for enhancing cellular compatibility and mouse myoblast i.e., C2C12 cells were used as a model cell for this study.

4.2 Materials and methods

4.2.1 Materials

C2C12 Mouse Myoblast cell line (NCCS, Pune, India), Dulbecco's Modified Eagle Medium (DMEM) high glucose, Fetal bovine serum (FBS), penicillin-streptomycin (100 µg/mL penicillin and streptomycin) and gelatin (cell culture tested) were received from Hi-Media. (3-Aminopropyl)-triethoxysilane (APTES, 97%), Glutaraldehyde solution (GA, 25 wt. % in H_2O), and Phosphate buffered saline (PBS, 10X) were received from Sigma (Merck) India.

4.2.2 Sol-gel synthesis of ZnO

The ZnO was prepared by the commonly used sol–gel procedure [214] as illustrated in Figure 4.1. In brief, 0.2 M zinc acetate dehydrate ($Zn(CH_3COO)_2.2H_2O$) was first mixed in 2-methoxyethanol ($C_3H_8O_2$) at 75°C with constant stirring for 1 h to yield a clear and homogeneous solution. Then, an equimolar (0.2 M) monoethanolamine (MEA) was added into the solution as the stabilizer and the stirring was continued for another 2 h. The formed ZnO sol-gel was aged for 24 h and filtered through the 0.22 µm pores size PVDF membrane filter (Millex-GV Syringe Filter, Sigma, India).

4.2.3 Sensor fabrication process

The process of fabricating ZnO thin film coated MSM biosensor is shown in Figure 4.2. In brief, single-side indium tin oxide (ITO) coated glass substrate (Film thickness = 150 nm) was cut with following dimensions 25 mm × 15 mm as shown in Figure 4.2a. The ITO coated glass substrate was covered using high temperature Teflon tape as shown in Figure 4.2b, in-order to develop a co-planar electrode system.

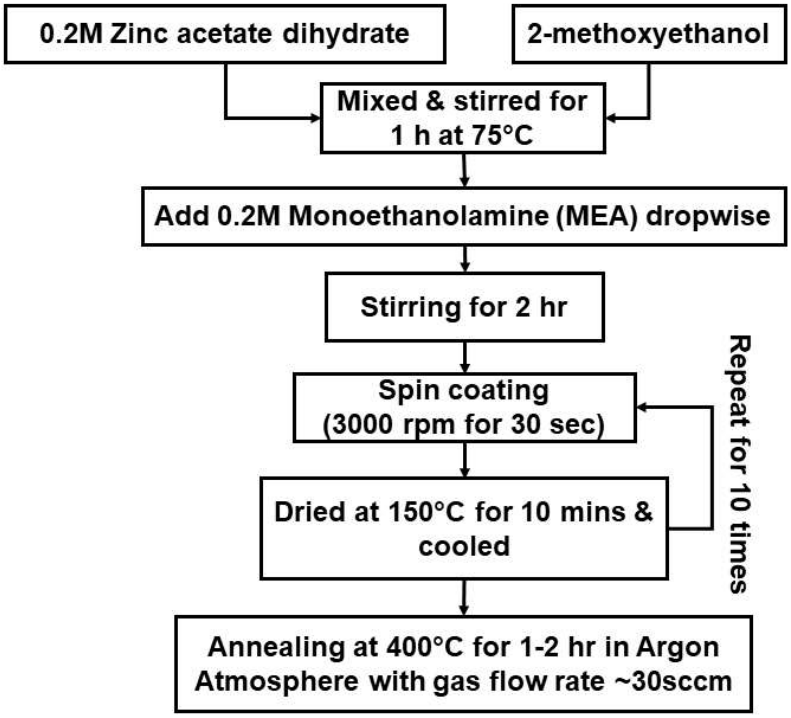

Figure 4.1: ZnO sol-gel preparation method and its spin coating process.

The uncovered ITO regions were etched-out using 9 M hydrochloric acid (HCl, 37%, Merck India) [215], to get an electrode dimension of 12 × 5 mm^2 at each side with a gap of 1 ± 0.2 mm (at centre) as shown in Figure 4.2c. The cleaned (etched ITO-coated glass and normal glass) substrates were coated using ZnO sol-gel solution. The rotation cycle of 3000 rpm for 30 s by spin coating technique was repeatedly used to achieve ∼100 nm film thickness. The coated ZnO film samples were heated at 150°C for 10 min at each steps to remove any organic residuals. Finally, the obtained ZnO film spin coated (etched ITO coated -glass and normal glass) substrates were annealed at 400 °C for 1-2 h in the inert (Argon) atmosphere (gas flow rate of about ∼30 sccm) in the muffle furnace in order to obtain crystallized ZnO thin film [77]. The fabricated MSM device is shown in Figure 4.2d.

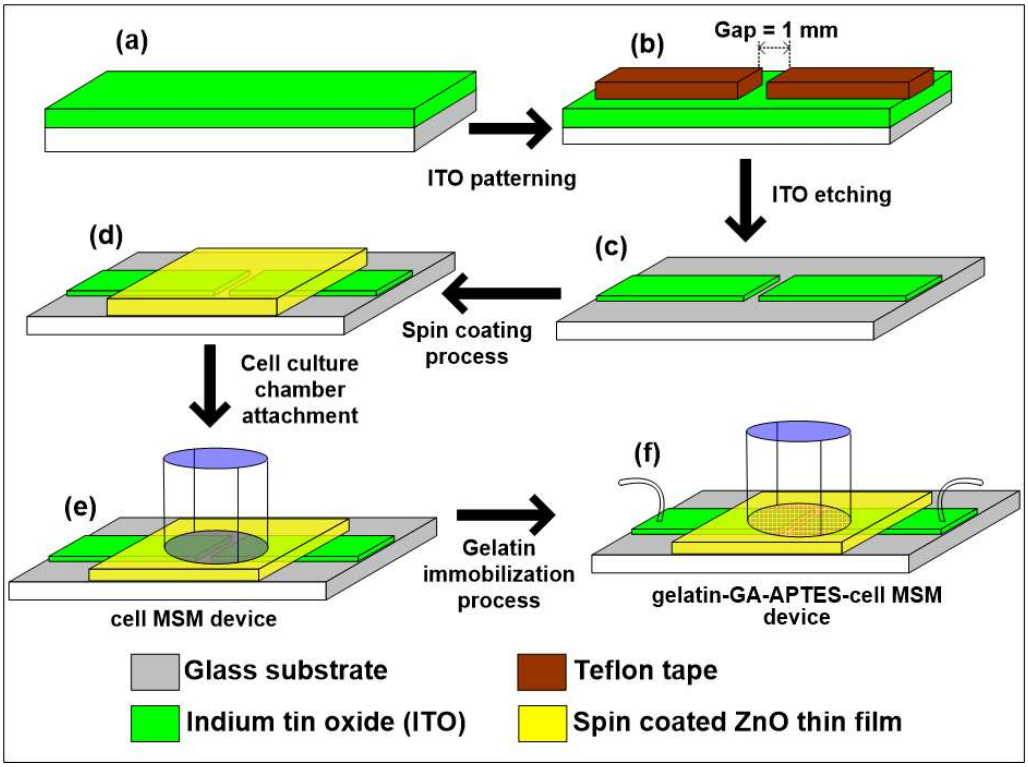

Figure 4.2: Transparent ZnO thin film coated MSM based biosensor fabrication process.

For maintaining the culture media, Cliklok Micro Centrifuge (Tarsons Product Pvt Ltd, India) tube was cut and used as **described section 2.2.2**, as shown in Figure 4.2e. The developed setup will be mentioned as cell MSM device in subsequent discussion.

4.2.4 Cell culture procedure

The fabricated gelatin functionalized MSM biosensor was used to grow the Mouse myoblast (C2C12) cells. The cells were seeded at a density of 1,000 cells/well and 5,000 cells/well. Ref **Section 2.2.3** for more detailed cell culture procedure. The cell study was done in triplicate (n= 3), and its average result was represented.

4.3 Results and discussion

4.3.1 Thin film characterization of spin coated ZnO device

The XRD pattern of spin coated ZnO thin film was obtained using XRD system (Rigaku, MiniFlex-600, Japan) at wavelength, $\lambda = 0.154$ nm. XRD pattern is recorded at diffraction angle 2θ from 20° to 80° at a scanning rate of 5° min^{-1}. The XRD pattern of the spin coated ZnO thin film shown in Figure 4.3a has all the respective peaks (±0.1°) similar to JCPDS file no: 00-089-1397, which confirmed that ZnO thin film has wurtzite structure [216] with an average strain (ε) and crystallite size of 6.11 x 10^{-3} and 29.31 nm, respectively as per W-H plot is given Figure 4.3b. Further we calculated the crystalline size, d-spacing, micro-strain, and dislocation density using equation 4.1, equation 4.2, and equation 4.3, respectively, which is presented in Table 4.1.

$$D = \frac{k\lambda}{\beta \cos\theta} \tag{4.1}$$

where 2θ is peak position, θ is the diffraction angle and β is its corresponding full width half maxima (FWHM)

$$\delta = \frac{1}{D^2} \tag{4.2}$$

where δ is the dislocation density

$$\varepsilon = \frac{\beta}{4\tan\theta} \tag{4.3}$$

where micro-strain (ε).

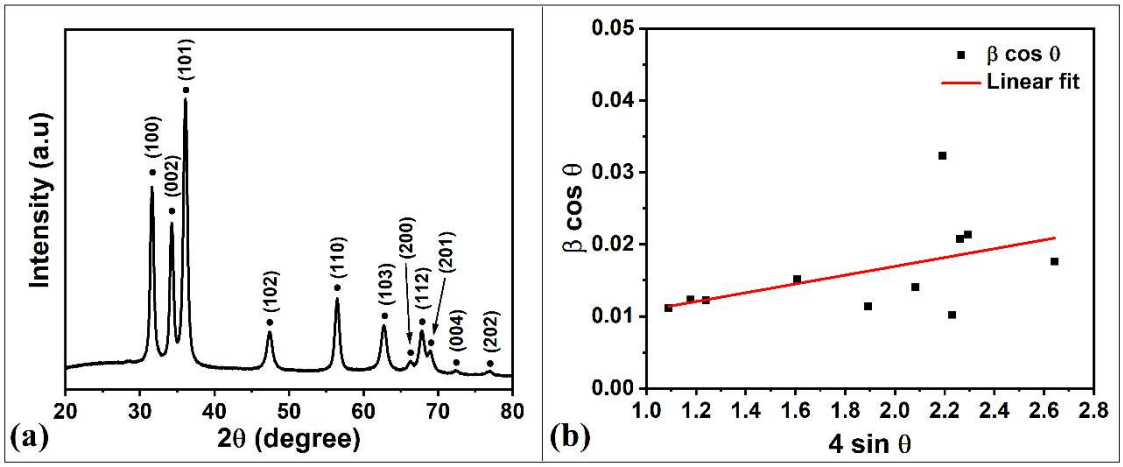

Figure 4.3: (a) XRD pattern of spin coated ZnO thin film, (b) Williamson-Hall (W-H) plot used for calculating average strain (ε) and crystallite size.

Table 4.1: Calculated XRD parameters.

Peak position (2θ)	**Peak width (2θ)**	**Scherer equation**	**Dislocation density**	**Micro-strain**	**Bragg equation**
		Crystallite size (nm)	**δ x 10^{-3} (nm^{-2})**	**ε x 10^{-3}**	**d-spacing (Å)**
31.614	0.666	12.400	6.503	10.262	2.828
34.256	0.739	11.244	7.910	10.468	2.616
36.077	0.738	11.317	7.808	9.892	2.488
47.383	0.948	9.148	11.949	9.430	1.917
56.457	0.741	12.171	6.751	6.022	1.629
62.720	0.943	9.869	10.268	6.749	1.480
66.456	2.212	4.293	54.253	14.734	1.406
67.793	0.706	13.559	5.439	4.584	1.381
68.864	1.443	6.676	22.434	9.182	1.362
70.020	1.491	6.504	23.642	9.290	1.343
82.680	1.345	7.865	16.168	6.673	1.166

The surface morphology of the ZnO thin film [217], [218] was investigated using AFM (NTEGRA Prima, NDT, Russia) in non-contacting mode (area 5 × 5 μm^2) and the obtained image is shown in Figure 4.4. From the obtained AFM image of the ZnO thin

film, it is found that the average roughness as 11.805 nm and it also confirms that the thin film formed is continuous without any gap. The surface morphology and its properties are evaluated and represented in the Table 4.2, as it is an important parameter which will determine the amount of mechanical stress induced on the functionality of adherent cells [68], [219]–[221].

The surface morphology of the ZnO thin film was investigated using AFM (NTEGRA Prima, NDT, Russia) and HR-SEM (Nova Nano SEM 450, FEI, US). The AFM was performed in non-contacting mode in 5 × 5 μm^2 area and the obtained image is shown in Figure 4.4. The average roughness of the ZnO thin film was calculated to be 11.805 nm, as it is considered to be one of the important parameters (Table 4.2) that play a key role in cellular adhesion and mechanobiology of the cells [9], [217], [218]. Further, from the AFM (Figure 4.4a) and HR-SEM images (Figure 4.4b), it was observed that the obtained spin coated ZnO thin film was continuous and fibrous in structure without any gap.

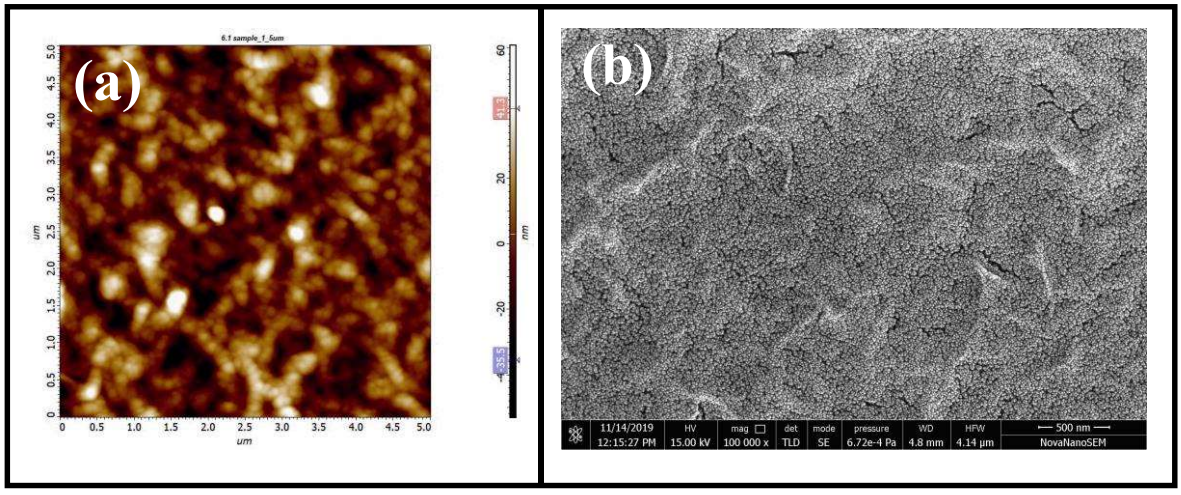

Figure 4.4: (a) AFM micrograph, and (b) HR-SEM image of spin coated ZnO thin film.

Table 4.2: Calculated AFM parameters.

AFM parameters	Values
Peak-to-peak	113.326 nm
Root mean square	14.854 nm
Roughness average	11.805 nm
Skewness	0.179
Kurtosis	3.089

The optical absorbance of the spin coated ZnO film was evaluated using UV-*Vis* spectroscopy (EI Instruments) at the wavelength ranging from 250 to 700 nm shown in Figure 4.5(a). The optical band gap of the ZnO film is calculated using equation 4.4 using Tauc plotting method [167] shown in Figure 4.5(b).

$$(\alpha h\nu) = B\left(h\nu - E_g\right)^{1/2} \tag{4.4}$$

where $h\nu$ corresponds to photon energy, α corresponds to absorption coefficient, E_g corresponds to optical bandgap and B is a constant. The optical bandgap of ZnO thin film was determined from the plot $(\alpha h\nu)^2$ *vs.* eV [222]. The E_g of the ZnO thin film was found to be 3.34 eV.

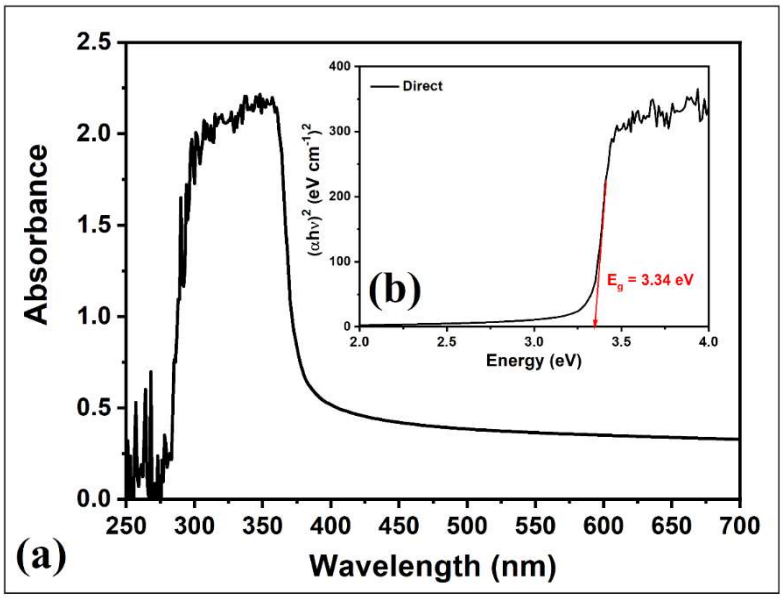

Figure 4.5: (a) Absorbance spectra, and (b) Tauc's plot of spin coated ZnO thin film.

The elemental composition of spin coated ZnO thin film was calculated using EDX (Team Pegasus Integrated EDS-EBSD with Octane Plus and Hikari Pro, EDX Inc, USA). The EDX pattern of spin coated ZnO thin film is shown in Figure 4.6, which confirmed the presence of ZnO in the fabricated device.

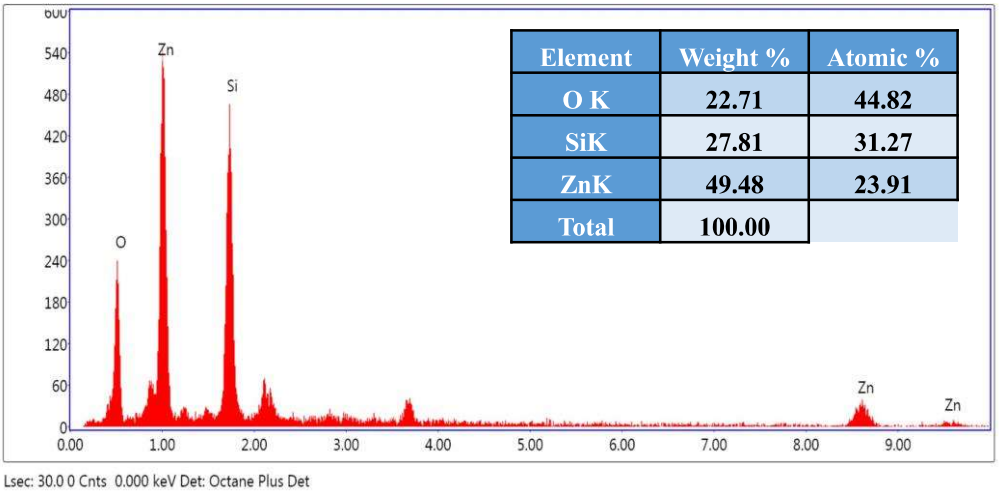

Element	Weight %	Atomic %
O K	22.71	44.82
SiK	27.81	31.27
ZnK	49.48	23.91
Total	100.00	

Figure 4.6: EDX pattern of spin coated ZnO thin film with elemental composition table.

4.3.2 Surface modification of ZnO thin film

The cell-membrane is made up of double layered phospholipids (which are considered to be amphiphilic), and are negatively charged. The phospholipid bilayer in the cell-membrane prevents the movement of ions/molecules in and out of the cell (by forming channels and the pumps selective towards the movement of particular ion or molecule) and separating the cell from the surrounding environment. The membrane also has some receptor proteins that allow the cell to respond to external signalling molecules (such as hormones) [70], [223]. The surface roughness and charge of the nanomaterial play an important role in cell-cell interaction as well as in governing other cellular functions. Hence, providing positively charged surface will modulates the cellular functions effectively at nanoscale topographical level [66], [176], [224], [225]. To achieve charged and effective cellular functions, we chose ZnO as the base material for fabricating MSM device and gelatin as an adhesive protein molecule. In brief, the ZnO nanomaterial is well-known for its polar Zn-O bonding, which is largely ionic (i.e., Zn^{2+}–O^{2-}) with corresponding radii of 0.074 nm and 0.140 nm respectively, and electrically charged due to the presence of zinc and oxygen planes [226]–[228]. Further gelatin is known to have inherent cell adhering moieties which will accelerate the cellular functions [176], [229].

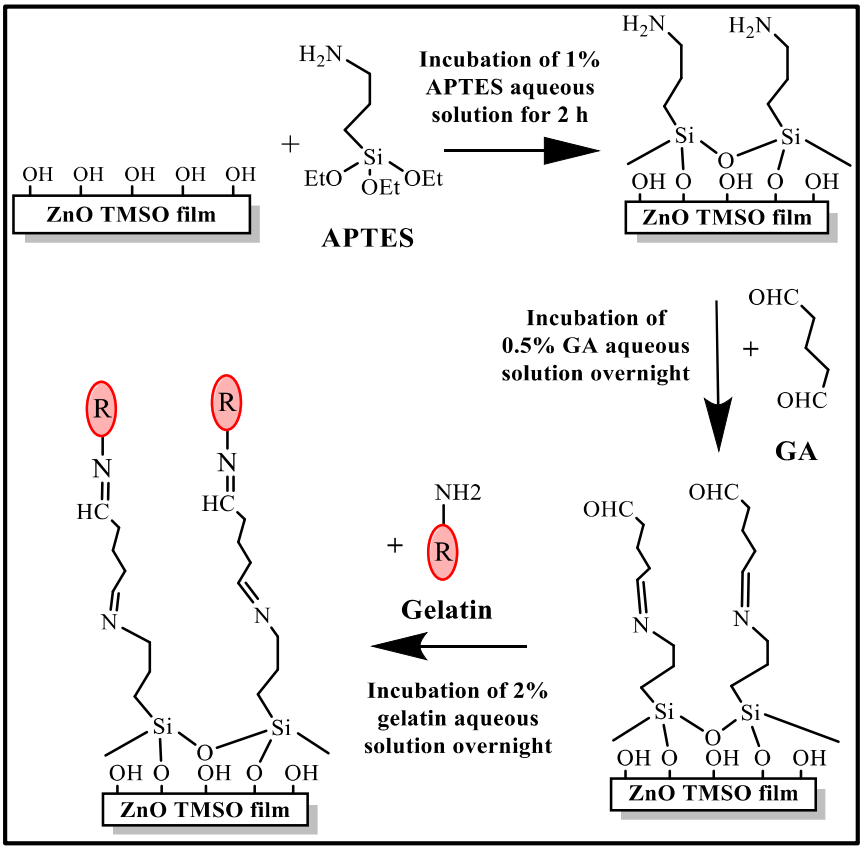

Figure 4.7: Schematic illustration of gelatin functionalization on spin coated ZnO thin film.

Here, the surface modification was done through chemical cross-linking method [225]. The cell MSM was cleaned using plasma cleaner (Model: Cute, Femto Science Inc, South Korea) at 10^{-2} mbar vacuum with a power of 50 W for 1 min to remove the presence of any organic contaminants [66], [224]. The plasma cleaned devices were then immediately incubated with 1% APTES aqueous solution for 2 h to form APTES-cell MSM (R-NH_2, amine functionalization) [224]. The APTES-cell MSM was then incubated with 0.5% GA aqueous solution for overnight to form GA-APTES-cell MSM (R-CHO, aldehyde functionalization as a linker to attached gelatin molecule) [225]. The GA-APTES-cell MSM was washed trice using 1X PBS solution, to eliminate the excess and unreacted molecules from the surface of the ZnO thin films. The GA-APTES-cell MSM was then

incubated with 2% gelatin aqueous solution for overnight, which form gelatin immobilized GA-APTES-cell MSM (protein functionalization) as shown in Figure. 4.7. The reaction was between amine (R-NH_2) functional group of adjacent lysine residues of gelatin molecule and two adjacent (R-OH) hydroxyl groups of APTES functionalized ZnO in the presence of glutaraldehyde crosslinker to form acetal bridges across the surface [225]. The gelatin immobilized GA-APTES-cell MSM can be referred as gelatin-GA-APTES-cell MSM. The gelatin-GA-APTES-cell MSM was then washed trice using 1X PBS solution, to eliminate the excess and unreacted (non-covalently linked) gelatin molecules/proteins from the surface of the ZnO films [229]. The gelatin-GA-APTES-cell MSM is shown in Figure 4.1f. Further, FT-IR analysis shown in Figure 4.8 was also performed to characterize and validate the surface functionalization of gelatin onto ZnO using Perkin Elmer IR spectrophotometer (Perkin Elmer Inc., USA). After the functionalization with gelatin, the fabricated MSM device was evaluated for its biocompatibility using MTT assay. The results showed that the ZnO thin film was completely biocompatible and able to support the cell proliferation efficiently (Figure 4.9).

4.3.2.1 Fourier Transform Infrared (FT-IR) spectroscopic study

FT-IR analysis was performed to characterize the surface functionalization of gelatin onto ZnO (Figure 4.8) using Perkin Elmer IR spectrophotometer (Perkin Elmer Inc., USA) in the transmittance mode at room temperature from 400 to 4000 cm^{-1} with a resolution of 2 cm^{-1} using the KBr pellet technique. The unmodified ZnO thin film (cell MSM) showed its characteristic peaks reveals that the peak at 3430, 1392, 1628, 2912 and 1027 cm^{-1} corresponds to O-H stretching, stretching vibrations of C=O, symmetric and asymmetric valency bands of C–H (i.e., CH_2 & CH_3), respectively. It also showed the peaks at 873

cm^{-1} and 436 cm^{-1} corresponds to Zn–OH and Zn–O respectively, which reflects the intensity of hydroxyl group present on the surface of the ZnO thin film [230], [231].

On the other hand, pristine gelatin showed its distinguished characteristic (zoomed image in Figure 4.8) 1st amide peak at ~1640 cm^{-1} corresponds to C=O and CN stretching, 2nd amide peak at 1538 and 1545 cm^{-1} corresponds to N-H bend, and C-H stretching, 3rd amide peak at 1243 cm^{-1} corresponds to C-N stretch with N-H in phase bending, with a CH_2 bending and wagging vibrational peaks at 1452 cm^{-1} and 1337 cm^{-1} respectively. A boarder amide peak at 3441 cm^{-1} corresponds to N-H vibration stretching, while a CH_2 asymmetric stretching vibration peak at 2932 cm^{-1} and a symmetric stretching vibration peak at 2848 cm^{-1}. Finally, at 1055 cm^{-1}, a CH_3 amide group is present with a C-O-C peak at 621 cm^{-1}[225], [232], [233].

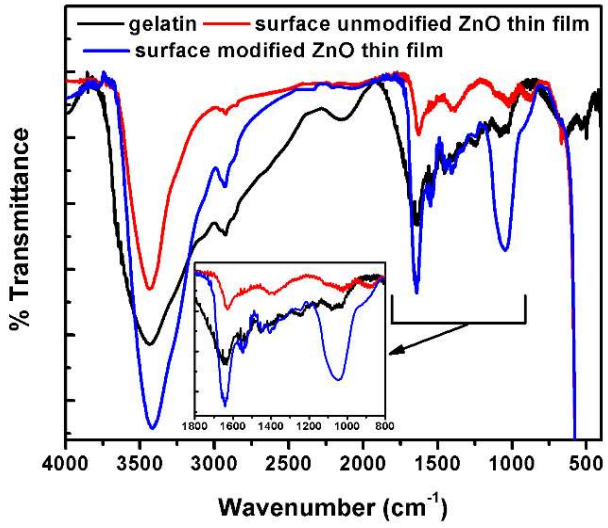

Figure 4.8: FT-IR spectra of pristine gelatin, surface unmodified ZnO thin film and surface modified ZnO thin film.

In the case of surface modified cell MSM, we observed a new peak at 1643 cm^{-1} corresponds to amide –CO-NH- stretching and there was a blue shift in the boarder peak at 3414 cm^{-1} corresponding to the amide stretch, which confirmed the modification of MSM with gelatin. Further the peak at 1054 cm^{-1} corresponds to Si-O-Si functional group,

which additionally suggested that the functionalization occurred due to the APTES in ZnO film.

4.3.2.2 Cell Viability and proliferation

For studying the cell viability [66], [176], [224], [225], gelatin-GA-APTES-cell MSM device (gelatin functionalized ZnO platform), cell MSM device (un-functionalized ZnO platform, as –ve control) and microwell attached glass cover slides (as +ve control) were used. The study was performed using MTT assay. Generally, a purple coloured formazan crystals is formed after the reduction of MTT (3-(4, 5 dimethylthiazol-2)-2, 5-diphenyltetrazolium bromide) by mitochondrial dehydrogenase enzyme in live cells. These formed formazan crystals are solubilized in DMSO solvent (or any appropriate solvent). The intensity of this solubilized formazan can be read using UV-*Vis* spectrophotometer that indicates the number of live cells at 570 nm. For the purpose, all the platforms (n = 5 each) were sterilized using 70% ethanol and UV light exposure before seeded the C2C12 cell lines of 5000 cells/well concentration and incubated at 37°C, 5% CO_2 under humidified conditions for 24 h, 48 h, 72 h, and 96 h. After incubation period, the culture media was thoroughly removed and 100 µL of MTT solution (5 mg/mL) in DMEM was added into the wells and incubated for 4h. After 4h, MTT solution was removed and 100 µL of DMSO was added and incubated again for another 1 h and then, the reading was taken at 570 nm in microplate reader (Synergy H1, Biotek, USA).

Figure 4.9 shows % of cell proliferation on the fabricated device. It was observed that there was a linear increase in the rate of measured cell proliferation for all the evaluated material. It was found that the gelatin functionalized MSM showed more percentage of proliferation rate; indicating proliferation of cells when cultured on the modified surface of materials. The plotting is performed by take 96 h positive (+ve) control as reference

point. During the cell adhesion process [69], [70] suspended cells in the cell culture chamber adhere on to materials' surface based on the surface topographical property of material with the help of focal adhesion transmembrane proteins, i.e., integrin, paxillin, vinculin, etc. It has been reported that the gelatin functionalization on the biomaterial improves cell-material interaction. It was also observed that the rate of cell proliferation in unmodified MSM was notably equivalent to unmodified glass [71], [234].

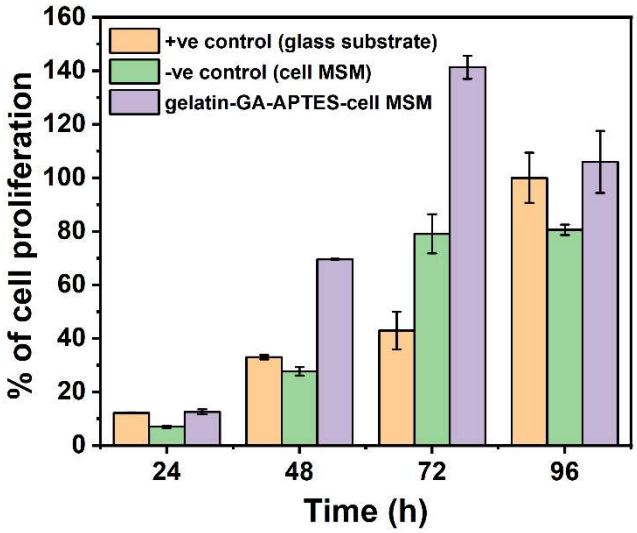

Figure 4.9: Cell viability and proliferation of C2C12 cells using MTT assay.

4.3.3 Electrical characterisation of fabricated cell MSM device

The MSM device was fabricated as depicted in Figure 4.2e. The fabricated cell MSM diode (n = 6) was characterized for the electrical performance using semiconductor parameter analyser (B1500A from Keysight, USA). Figure 4.10a shows the current-voltage *(I-V)* characteristics and confirmed the linear current response correspond to the applied voltage. The linear responses were due to formation of ohmic contact between ZnO and ITO without any significant interference between barrier as seen from band diagram (Figure 4.10b). It is known that under thermal equilibrium the charge carriers move efficiently through the junctions. The ohmic behaviour in the electrical

characteristics of the fabricated MSM were also verified using three dimensional (3D) simulation of the device in the ATLAS software (Silvaco, USA). The input parameters considered for the simulation are listed in Table 4.3 [235]. The obtained *I-V* characteristics are shown in Figure 4.10a as red line with circular dots.

Table 4.3: Parameters used for the simulation of ITO/ZnO/ITO device.

Parameters	**Values**
Effective density of states in the conduction band of ZnO (N_C) [cm^{-3}]	2.2×10^{18}
Effective density of states in the valance band of ZnO (N_V) [cm^{-3}]	1.8×10^{19}
Electron affinity of ZnO (χ) [eV]	4.35
Bandgap of ZnO (Eg) [eV]	3.37
Recombination lifetime for ZnO (τ_n and τ_h) [s]	2.1×10^{-9}
Donor concentration in ZnO (N_D) [cm^{-3}]	3.5×10^{14}
Dielectric constant of ZnO (ε)	9
Electron mobility in ZnO (μ_n) [cm^2/Vs]	100
Hole mobility in ZnO (μ_p) [cm^2/Vs]	25
Work function of ITO (ψ_m) [eV]	4.5

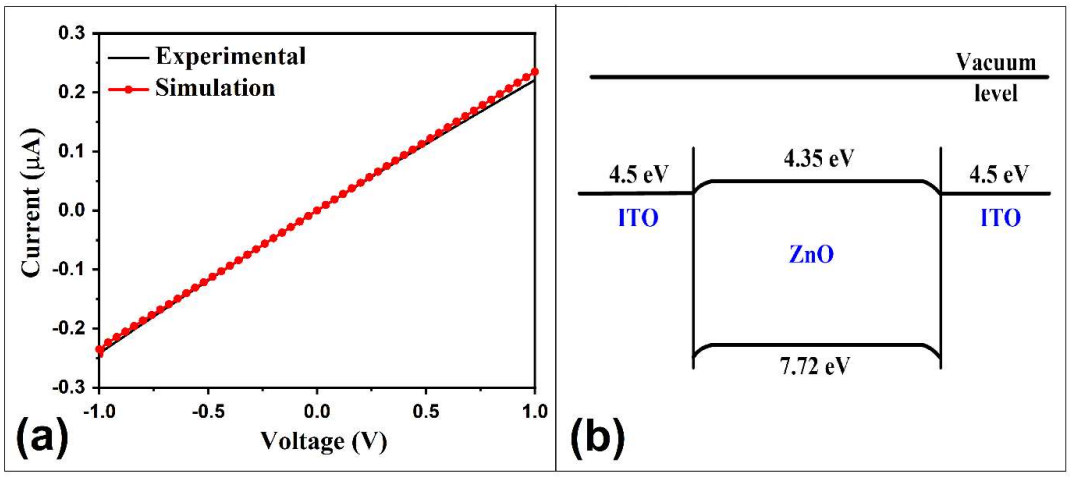

Figure 4.10: (a) *I-V* characteristics of fabricated and simulated MSM device (b) Band diagram for the device structure.

4.3.4 Optical and electrical characterisation of fabricated gelatin-GA-APTES-cell MSM device

We performed the cellular study by seeding cells of different concentration such as 1000 cells/well and 5000 cells/well into the culture chamber, to analyze the effect of cell-substrate interaction in terms of change in the electrical (dielectric) properties i.e., change in resistance, capacitance or impedance with respect to the time over each concentration of the cells seeded. Figure 4.11a shows cells grown in the device after 6 h, It was observed that, cells became flat, which implied that the cells sensed its appropriate surface; adapted to the microenvironment and started to grow on ZnO based MSM device [223]. The experiments were done in triplicate (n = 3) and the average data were represented. We carried out both optical and electrical measurements at every 24 h time interval, in order to avoid disturbance in the cells growing biological environment.

4.3.4.1 Case 1-1000 cells/well concentration

Figure 4.11a-f shows the cell proliferation in MSM device with the cell density of 1000 cells/well using a bright field microscope for different time-interval. We observed significantly improved cell proliferation on MSM gelatin functionalized substrate compared with the unmodified MSM substrate. We observed an increase in magnitude of the impedance with an increase in cell number with respect to time until 72 h. It was observed that, when the cells drifted downwards and started adhering to the surface of the device (i.e., thin film), a significant level of alteration in the current flow happened, which caused a change in the dielectric properties of the fabricated device (i.e., thin film) as shown in Figure 4.12. However, after 72 h, we observed that there was a significant decrease in the number of cells as seen from microscopic images (Figure 4.11); most likely due to differentiation of live myoblast cells to form myotubes. Due to which the

myoblast cells undergoing differentiation eventually gets detached from the substrates to develop into fully mature [84], [175].

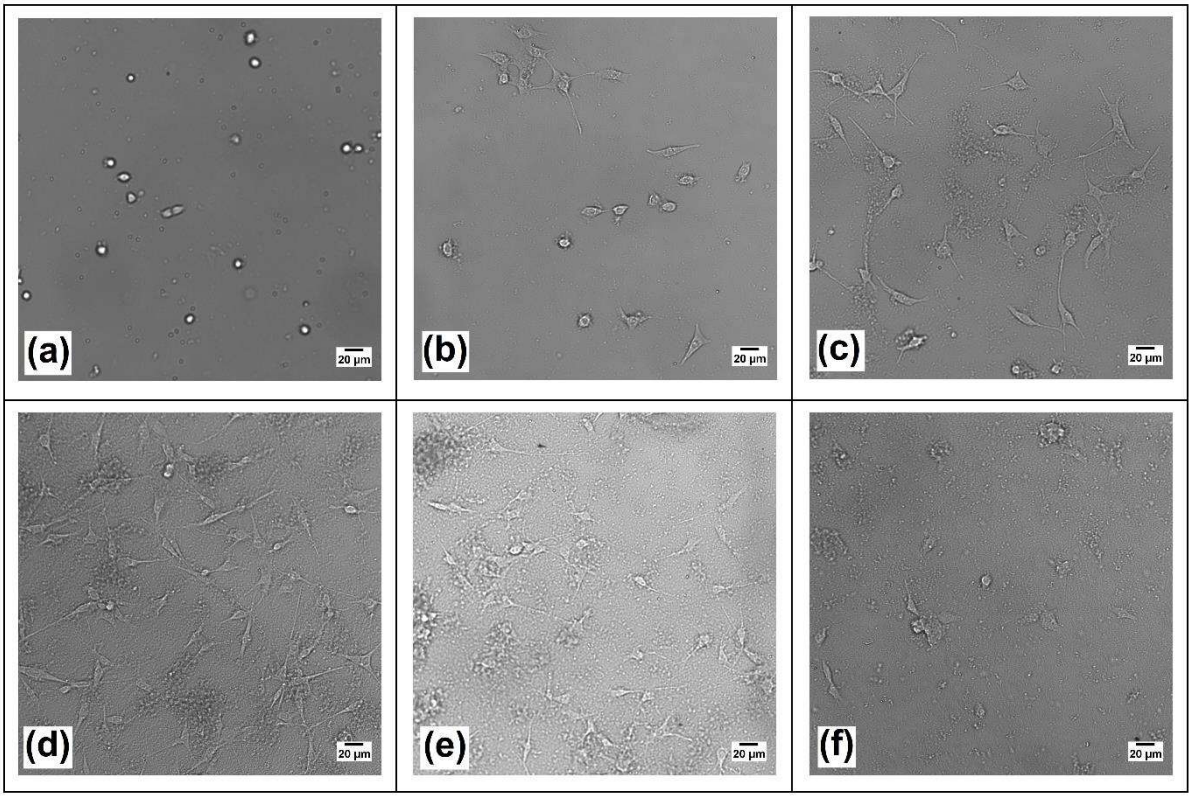

Figure 4.11: Morphological changes of C2C12 cells at various time: (a) 6 h, (b) 24 h, (c) 48 h, (d) 72 h, (e) 96 h, and (f) 120 h; Scale bar: 20 µm.

At the higher frequency, the depth of penetration of an AC signal is very high, hence the measured impedance or capacitance is due to the flow of charges through the intercellular region of the biological cells. However, with the decrease in operating frequency, the measured impedance and capacitance are due to contribution of charge flow through the extracellular and intercellular regions of the biological cells. Hence, the characteristics of current flowing ability and capacitive property of the fabricated device are measured as shown in Figure 4.12a & b. The results revealed that the current and capacitance are decreased as the cells underwent adhesion and progressed for the other cellular function, such as proliferation and differentiation after 72 h as shown in Figure 4.11e and Figure

4.12c. A change in the shape of phase angle shown in Figure 4.12d was observed as the cellular functions progressed owing to the cell-substrate and cell-cell interactions [175].

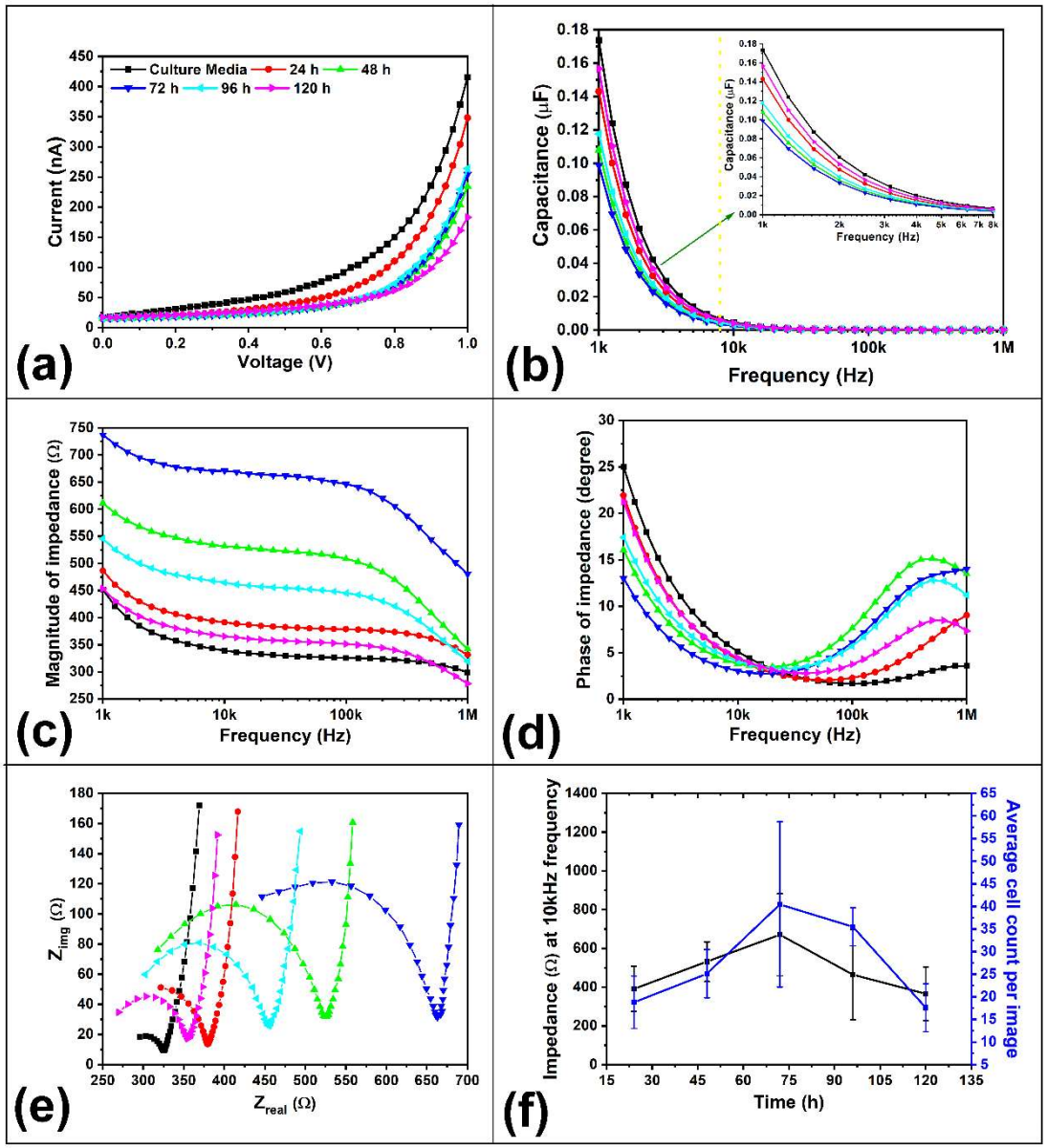

Figure 4.12: Electrical properties of the ZnO thin film with respect to change in cell proliferation (1000 cells seeded): (a) *I-V* characteristics plot, (b) Capacitance *vs.* frequency plot, (c) Magnitude of impedance plot, (d) Phase of impedance plot, (e) Nyquist plot, and (f) Time *vs.* change in impedance and average cell count plot.

The deviation in the semi-circle of the Nyquist plot shown in Figure 4.12e could be due to the change in impedance of the constant phase element (Z_{CPE}) [79], [99] and the Z_{CPE} dependent on double-layered capacitance (Q_{dl}), which was modulated by the empirical

parameter 'n' [79]. Therefore, here the change in the diameter of the semi-circle was due to the cell proliferation and a decrease in diameter of the semi-circle was due to the decrease in the availability of cells on the MSM substrate. Thus, the outcomes suggest that the fabricated device can provide changes in an electrical parameter corresponding with the progression of cellular processes exhibited by the adherent mammalian cells. On the other hand, the average cell count at different time interval is shown in Figure 4.12f.

4.3.4.2 Case 2-5000 cells/well concentration

Since the number of cells seeded per well was relatively more, there may be a possibility that we could observe the minute changes in the electrical parameters resulting from the cell-cell and cell-substrate interactions which otherwise may not be possible to observe at a lower cellular density. We observed that both the microscopic images and electrical measurements in case 2 were correlating well each other. The increase in the rate of cellular proliferation over different time interval is shown in Figure 4.13a-h. We observed a noticeable decrease in current flowing ability as shown in Figure 4.14a and capacitance value as shown in Figure 4.14b for the fabricated devices (upto 144 h). The changes in current and capacitance are due to a significant increase in the impedance of the fabricated device as shown in Figure 4.14c. The respective changes in the shape of phase angle due to cellular functions are shown in Figure 4.14d.

Further, from Nyquist plot shown in Figure 4.14e, it can be observed that the dielectric properties of the fabricated device get altered with the progression of cellular functions over time; as the true impedance of the semiconducting materials gets increased with a noticeable shift towards the higher resistance while a significant increase in the semi-circle diameter. The average cell count shown in Figure 4.14f were observed till 120 h followed by a noted decrease in both parameters observed until 168 h most likely due to the differentiation of myoblast cells (i.e., exit from cell cycle to form myotubes). The outcomes indicate that the sufficient number of cells is required on the substrate for the

cell-cell interaction to take place as well as to produce myotubes within the duration 120 h to 168 h, as observed through the microscopic examinations.

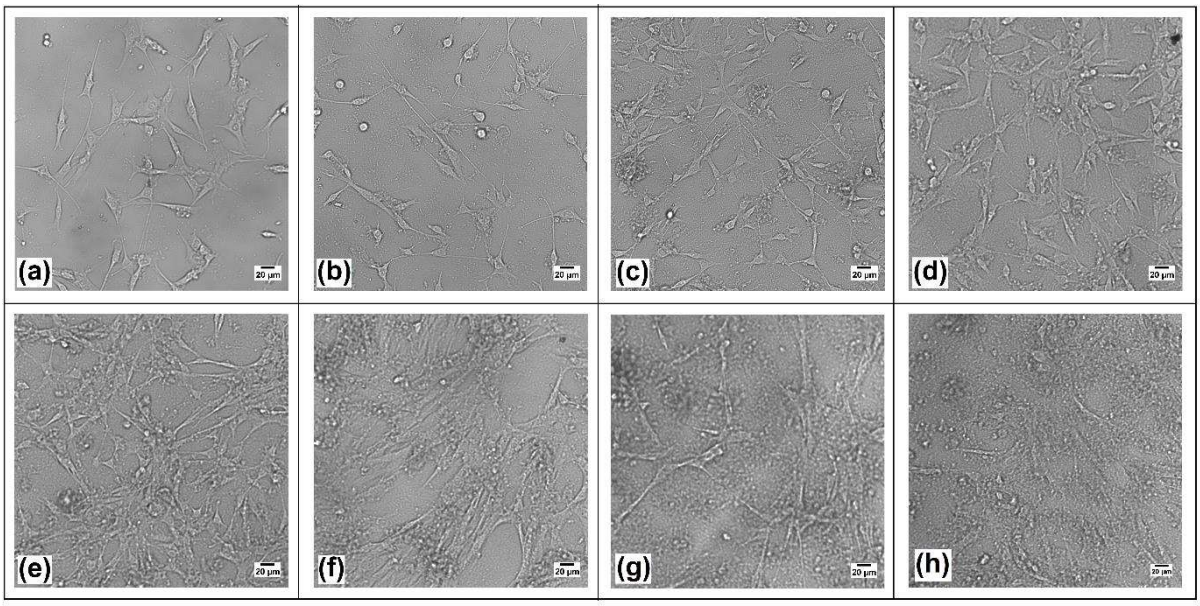

Figure 4.13: Morphological changes of C2C12 cells at various time: (a) 24 h, (b) 48 h, (c) 72 h, (d) 96 h, (e) 120 h, (f) 144 h, (g) 168 h, and (h) 210 h ; Scale bar: 20 μm.

Such observation is further supported by a noted increase in current flow with a gradually decrease in impedance between 144 h to 168 h with a change in phase angle shown in Figure 4.14c. After 168 h (i.e., up to 210 h), the cells started to detach from the surface as observed in microscopic images shown in fig 4.13. This may be attributed to the possibility of formation of mature myotubes within this duration. Thus, it can be further inferred that the progression of cellular processes modulates with the variation in the cell density which is found well in coherence with the change in the electrical parameters.

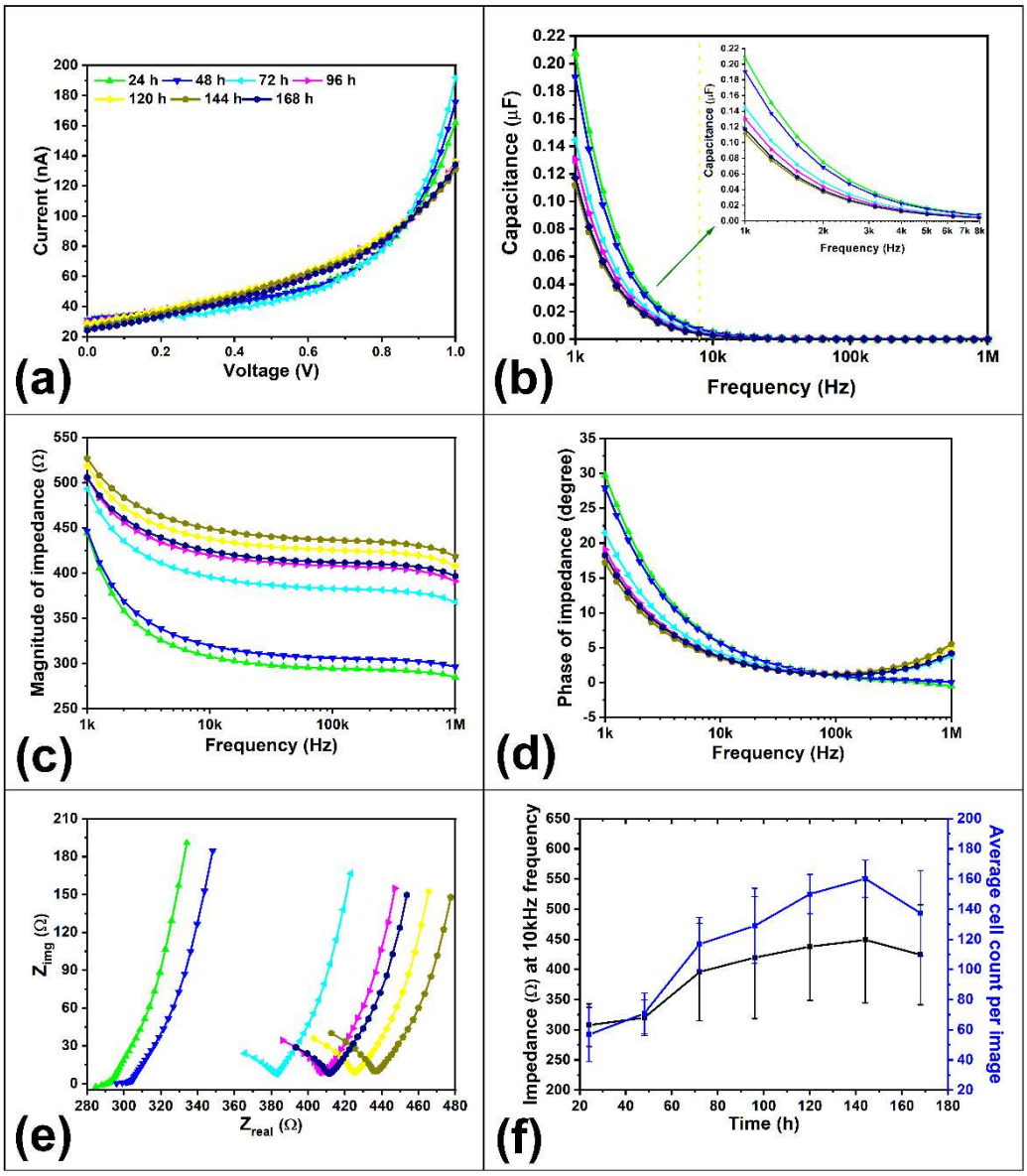

Figure 4.14: Electrical properties of the ZnO thin film with respect to change in cell proliferation (5000 cells seeded): (a) *I-V* characteristics plot, (b) Capacitance *vs.* frequency plot, (c) Magnitude of impedance plot, (d) Phase of impedance plot, (e) Nyquist plot, and (f) Time *vs.* change in impedance and average cell count plot.

4.4 Conclusion

In the present work, we have demonstrated that modulation of the dynamic behaviour of the adherent mammalian cells using electrical properties of the ZnO based semiconducting nanomaterial. This work reports the analysis of cellular processes using

the fabricated gelatin functionalized ZnO based MSM device with respect to the change in electrical response using a unique biosensing platform. The obtained results based on the electrical parameters are well in correlation with the functional changes in the cellular processes as observed through microscopic images and MTT assay. Further, the dynamic behaviour of adherent mammalian cells is analyzed by optimizing the appropriate cell density. Therefore, the ZnO thin film based MSM biosensor could be used for various biosensing applications wherein dynamic changes of the cells play a vital role.